Transabdominal contrast-enhanced ultrasound imaging of the prostate

Ultrasound in Med. & Biol., Vol. 41, No. 4, pp. 1112–1118, 2015

0301-5629/$ - see front matter

http://dx.doi.org/10.1016/j.ultrasmedbio.2014.10.014

● *Technical Note*

TRANSABDOMINAL CONTRAST-ENHANCED ULTRASOUND IMAGING OF THE PROSTATE

Massimo Mischi,* Libertario Demi,* Martijn Smeenge,† Maarten P. J. Kuenen,*† Arnoud W. Postema,† Jean J. M. C. H. de la Rosette,† and Hessel Wijkstra*†

*Electrical Engineering Department, Eindhoven University of Technology, Eindhoven, The Netherlands; and †Urology Department, Academic Medical Center, University of Amsterdam, Amsterdam, The Netherlands

(*Received* 30 *June* 2014; *revised* 22 *October* 2014; *in final form* 24 *October* 2014)

Abstract—Numerous age-related pathologies affect the prostate gland, the most menacing of which is prostate cancer (PCa). The diagnostic tools for prostate investigation are invasive, requiring biopsies when PCa is suspected. Novel dynamic contrast-enhanced ultrasound (DCE-US) imaging approaches have been proposed recently and appear promising for minimally invasive localization of PCa. Ultrasound imaging of the prostate is traditionally performed with a transrectal probe because the location of the prostate allows for high-resolution images using high-frequency transducers. However, DCE-US imaging requires lower frequencies to induce bubble resonance and, thus, improve contrast-to-tissue ratio. For this reason, in this study we investigate the feasibility of quantitative DCE-US imaging of the prostate via the abdomen. The study included 10 patients (age = 60.7 ± 5.7 y) referred for a needle biopsy study. After having given informed consent, patients underwent DCE-US with both transabdominal and transrectal probes. Time–intensity contrast curves were derived using both approaches and their model-fit quality was compared. Although further improvements are expected by optimization of the transabdominal settings, the results of transabdominal and transrectal DCE-US are closely comparable, confirming the feasibility of transabdominal DCE-US; transabdominal curve fitting revealed an average determination coefficient $r^2 = 0.91$ ($r^2 > 0.75$ for 78.6% of all prostate pixels) compared with $r^2 = 0.91$ ($r^2 > 0.75$ for 81.6% of all prostate pixels) by the transrectal approach. Replacing the transrectal approach with more acceptable transabdominal scanning for prostate investigation is feasible. This approach would improve patient comfort and represent a useful option for PCa localization and monitoring. (E-mail: M.mischi@tue.nl) **© 2015 World Federation for Ultrasound in Medicine & Biology.**

Key Words: **Prostate cancer, Contrast-enhanced ultrasound, Ultrasound contrast agents, Dilution curve, Transabdominal ultrasound, Transrectal ultrasound, Perfusion.**

INTRODUCTION

Prostate problems are a major age-related burden in men. Three in four men in their sixties present with lower urinary tract symptoms, which are often the result of benign prostate hyperplasia (Wei et al. 2008), but generate concerns for prostate cancer (PCa) and thus require special investigations (Brown et al. 2003). PCa is the cancer with the highest incidence in Western men (Siegel et al. 2014). Twenty-seven percent of all new malignancies diagnosed in men in 2014 in the United States are expected to be prostate cancer (Siegel et al. 2014). Standard PCa diagnosis comprises digital rectal examination, assessment of serum prostate-specific antigen levels and transrectal ultrasound (TRUS) imaging. All have serious limitations: digital rectal examination is subjective and assesses only a part of the gland (the posterior part), whereas the prostate-specific antigen test is not disease specific, producing about two in three false-positive results (Draisma et al. 2003; Schröder et al. 2009). Ultrasound is the most used clinical instrument for pre- and peri-operative visualization of the prostate gland. It permits estimation of the prostate volume, as well as guidance for systematic biopsies. In addition, gray-scale and Doppler imaging may provide diagnostic information on intraprostatic abnormalities, although its poor sensitivity and specificity make this approach unreliable (Aarnink et al. 1998; Sedelaar et al. 2001).

Because of the relatively small size of the prostate and its proximity to the rectal wall, prostate imaging is

Address correspondence to: Massimo Mischi, Electrical Engineering Department, Eindhoven University of Technology, Room PT 3.02, P.O. Box 513, 5600 MB Eindhoven, The Netherlands. E-mail: M.mischi@tue.nl

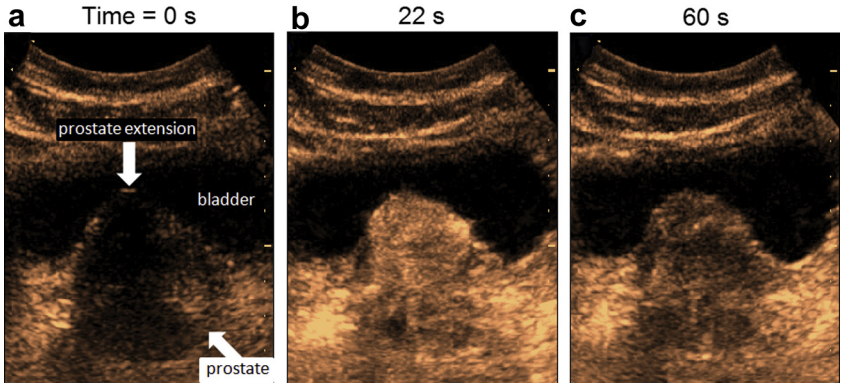

Fig. 1. Three selected frames from the transabdominal dynamic contrast-enhanced ultrasound scan (a) before ultrasound contrast agent wash-in, (b) at peak concentration and (c) during washout, revealing a hypervascularized prostate extension toward the bladder. The bladder, prostate and a prostate extension into the bladder are indicated in (a).

conventionally performed with a transrectal probe that allows use of high-frequency ultrasound (typically >8 MHz) to provide high-resolution images. The quality of the images justifies the patient's discomfort caused by transrectal access.

More recently, the potential of advanced imaging methods, including elastography and dynamic contrast-enhanced ultrasound (DCE-US) imaging, to improve detection and localization of PCa has been reported (Salomon et al. 2008; Wink et al. 2008). Elastography estimates tissue stiffness as a marker for increased cellular density and, therefore, cancer (Salomon et al. 2008). DCE-US can detect signals from the microvasculature and serves as a marker for neoangiogenesis and tumor progression (Halpern et al. 2001; Russo et al. 2012). This relates to the diameter of the microbubbles used as ultrasound contrast agents (UCAs); they are gas microbubbles with a size comparable to that of red blood cells (Schneider 1999) and can therefore flow through the smallest microvessels. A large retrospective study reported that UCAs are tolerable for non-cardiac applications (Piscaglia et al. 2006).

Several methods have been proposed for detection of changes in the microvascular architecture based on the assessment of tissue perfusion by analysis of the time evolution (wash-in and wash-out) of the UCA concentration (Russo et al. 2012). To this end, specific (empirical) features are estimated from UCA time–intensity curves (TICs) measured after a peripheral intravenous injection of an UCA bolus (Eckersley et al. 2002). Typical features extracted are the mean transit time, wash-in rate and area under the curve. More recently, some authors have proposed UCA dispersion as a better marker than perfusion for detection of angiogenic changes in the microvascular architecture (Kuenen et al. 2011). The results obtained in the prostate are promising and have motivated the development of improved algorithms for dispersion analysis (Kuenen et al. 2013b; Mischi et al. 2012).

Driven by established clinical practice and the common thought that a transrectal approach leads to improved spatial resolution, DCE-US has always been performed by TRUS, but this overlooks essential technical aspects of the imaging system. In particular, DCE-US is performed with contrast-specific imaging using dedicated pulse schemes that improve microbubble detectability by suppressing tissue echoes and thus increasing the contrast-to-tissue ratio (Frinking et al. 2000). Commonly used solutions for contrast-specific imaging modes aim at enhancing the non-linear signals produced by UCAs compared with the linear signals produced by tissue (Frinking et al. 2000).

An important feature common to all these methods relates to the chosen ultrasound frequency; to achieve strong contrast signals, the ultrasound frequency should be close to the resonance frequency of the microbubbles used. According to microbubble simulations and dedicated measurements, the resonance frequency of commercially available UCAs is ≤3 MHz (Fillon 2013; Gorce et al. 2000; Schneider 1999). Therefore, when TRUS is used, the high US frequencies that are allowed by the small imaging depth (low attenuation) are lowered to values that are close to the microbubble resonance frequency. This permits achievement of efficient contrast enhancement at the cost of a lower spatial resolution.

In the work described here we evaluated for the first time the feasibility of DCE-US imaging of the prostate via the abdomen, using lower frequencies that are close to the microbubble's resonance and permit achievement of the required, greater depth. To this end, the quality of TICs acquired by transabdominal scanning is evaluated and compared with that of TICs acquired by a transrectal probe. The transabdominal approach avoids patient discomfort and simplifies clinical practice.

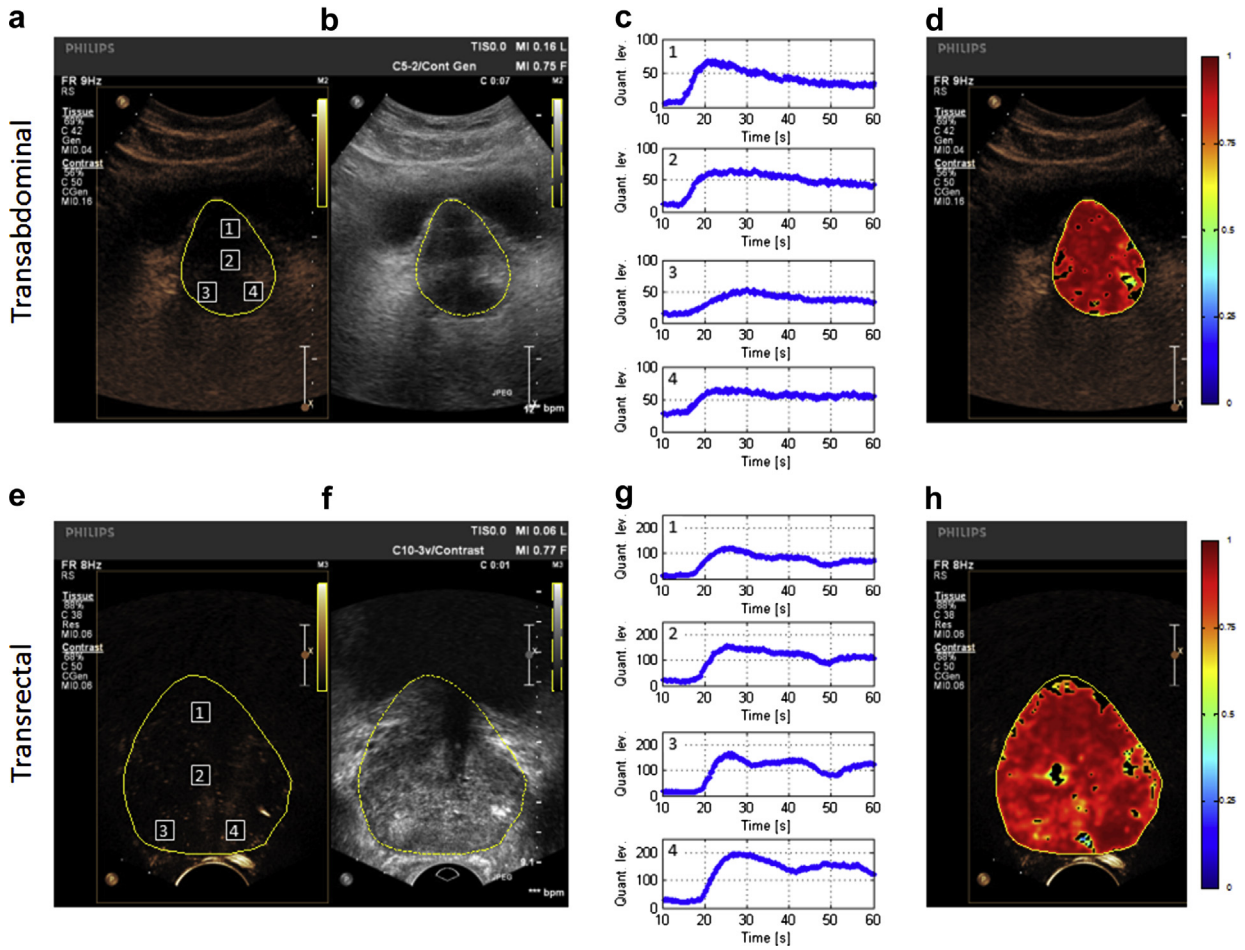

Fig. 2. Transabdominal (top) and transrectal (bottom) contrast-enhanced (a, e) and fundamental (b, f) scans of the patient in Figure 1 with four overlaid regions of interest (a, e) where the displayed time–intensity curves (c, g) have been measured. Clear time–intensity curves can be extracted in different regions throughout the entire prostate gland. The corresponding parametric (color) maps displaying the determination coefficient r^2 of the local density random walk model fit to time–intensity curves measured at each pixel are shown on the right (d, h).

METHODS

The study was institutional review board approved and included patients referred for a needle biopsy study. After having given informed consent, patients underwent the DCE-US investigations.

Patients underwent both transrectal and transabdominal DCE-US scans of the prostate in random order before biopsy. The patients were asked not to void before the scans to avoid an empty bladder and, therefore, the presence of additional (attenuating) tissue along the path between the transabdominal probe and the prostate. For each scan, a 2.4-mL SonoVue (Bracco SPA, Milan, Italy) UCA bolus was administrated intravenously followed by a 5-mL saline flush, and the transit of the bolus through the prostate was imaged and recorded using an iU22 ultrasound scanner (Philips Healthcare, Bothell, WA, USA). C10-3v and C5-2 probes were used for the transrectal and transabdominal scans, respectively. TIC acquisition requires an approximately 1-min recording during which the ultrasound probe must be kept still to obtain TICs that are derived from one tissue plane and are not affected by motion artifacts.

The acquired contrast ultrasound image sequences were stored in the digital imaging and communications in medicine (DICOM) format and analyzed off-line in MATLAB (The MathWorks, Natick, MA, USA) to evaluate the quality of the recorded data.

Patients

Ten patients (age = 60.7 ± 5.7 y) were included. The patients had body mass index ranging from 21.5 to 35.5 kg/m^2, a prostate volume from 16 to 145 mL and a prostate-specific antigen level from 0.6 to 42.2 ng/mL. Because of an evident hypervascularized prostate

Table 1. Statistics of the determination coefficient r^2 of the local density random walk fits to time–intensity curves measured by TA and TR dynamic contrast-enhanced ultrasound at each pixel covering the prostate

	r^2		$r^2 > 0.75$ (%)		Failed fit (%)	
Patient	TA	TR	TA	TR	TA	TR
1	0.93 ± 0.10*	0.90 ± 0.11	83.7	86.0	10.0	6.8
2	0.92 ± 0.13	0.91 ± 0.10	69.5	87.0	12.5	6.1
3	0.90 ± 0.15	0.92 ± 0.13	76.6	83.7	9.3	8.6
4	0.96 ± 0.07	0.92 ± 0.09	86.0	86.6	10.9	7.8
5	0.88 ± 0.12	0.91 ± 0.11	67.9	82.1	21.0	9.8
6	0.92 ± 0.11	0.95 ± 0.08	77.3	91.2	16.0	5.4
6	0.90 ± 0.12	0.88± 0.12	76.7	68.8	13.8	21.0
7	0.93 ± 0.08	0.88 ± 0.14	93.8	76.7	2.1	10.1
9	0.87 ± 0.15	0.87 ± 0.14	66.0	70.5	19.0	16.7
10	0.90 ± 0.15	0.91 ± 0.12	83.4	86.6	8.0	5.0
Global†	0.91 ± 0.13	0.91 ± 0.12	78.6	81.6	12.4	10.1

TA = transabdominal; TR = transrectal.
* Mean ± standard deviation.
† Global values refer to the statistics over the complete set of time–intensity curves from all the scanned patients.

extension into the bladder base, providing a clear, common landmark to compare the transabdominal and transrectal scans, the patient in Figure 1 is taken as guiding example. This patient (age = 59 y) had a body mass index, prostate volume and prostate-specific antigen level of 35.5 kg/m^2, 98 mL and 42.2 ng/mL, respectively. Twelve of 12 biopsies were found positive with a Gleason score of 5 + 4.

Scanner settings

The acquisitions were performed in contrast-specific (power modulation) mode at 3.5 MHz with a mechanical index of 0.06 for the transrectal scan and at 1.7 MHz for the transabdominal scan with a higher mechanical index (0.16) to improve signal strength while maintaining a sufficiently low acoustic pressure so as to minimize bubble destruction (Frinking et al. 2000). For both the transrectal and transabdominal scans, the gain and the dynamic range were adjusted so that signal from tissue was slightly above the background level. As an example, in Figure 1 are three frames from the dynamic abdominal scan before UCA arrival, at peak concentration and during washout.

Quality measure

Time–intensity curves were extracted from the data sets obtained to evaluate the feasibility of performing DCE-US transabdominal imaging of the prostate compared with transrectal DCE-US imaging. Only TICs representing the prostate were extracted and evaluated. To this end, the prostate contour was determined by an expert and manually overlaid on the images.

Time–intensity curves were first measured in several regions of interest placed in both the peripheral and transition zones of the prostate for visual comparison of the transrectal and transabdominal data sets. A quantitative evaluation of TIC quality was performed by assessment of the signal-to-noise ratio, defined according to Mischi et al. (2007) as the ratio between the TIC peak and the noise standard deviation expressed in decibels.

Dynamic contrast-enhanced ultrasound quantification typically involves model fitting; therefore, the quality measure we adopted was the suitability of the recorded data for accurate model fitting. Before this, the data was linearized (Kuenen et al. 2011). We used the local density random walk model, which describes the convection–dispersion process of the microbubbles and is extensively reported to produce accurate fits of TICs (Mischi et al. 2003; Strouthos et al. 2010). The model-fitting algorithm proposed in Kuenen et al. (2011) was adopted. At each pixel in the prostate, the fit quality was assessed by the determination coefficient r^2, which is commonly used to indicate the agreement between a model and the data (Menard 2000). Color maps of r^2 were derived for both the transabdominal and transrectal scans to compare the quality of the data sets.

RESULTS

Figure 2 illustrates the results from the transabdominal and transrectal scans of the selected patient in Figure 1. Contrast-specific (Fig. 2a, e) and fundamental (Fig. 2b, f) images, as displayed by the scanner, are provided. The displayed TICs (Fig. 2c, g), which are derived in several regions of interest representative of different prostate zones, show comparable quality for the transabdominal and transrectal acquisitions, with the transabdominal TICs having lower amplitudes compared with the corresponding transrectal TICs. Single-pixel TICs measured in the same regions of interest had average signal-to-noise ratios equal to 18.77 ± 4.18 and 18.56 ± 3.10 dB for the transabdominal and the transrectal acquisitions, respectively. Parametric maps of the determination coefficient r^2 of the local density random walk fits to the TICs measured at each pixel covering the prostate are also provided (Fig. 2d, h). Pixels where no r^2 color is shown correspond to "failed fitting" because of poor or absent signals, caused, for example, by calcifications (no perfusion). Quantitative results for each patient are summarized in Table 1.

DISCUSSION

The comparison of transabdominal and transrectal data indicates the feasibility of transabdominal contrast-enhanced ultrasound imaging of the prostate. TIC quality that is adequate for quantitative analysis was achieved in all patients, with a wide range of body mass indexes and prostate volumes.

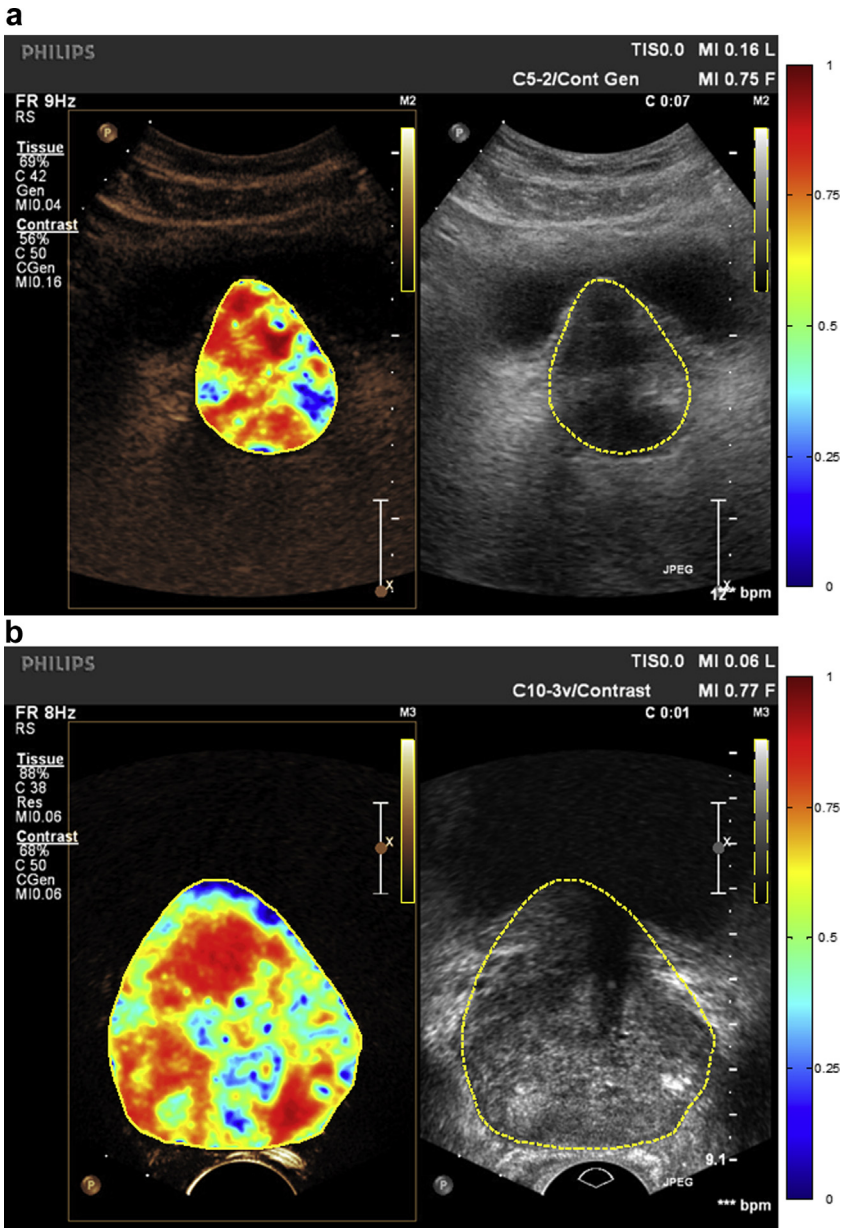

Fig. 3. Functional images of dispersion estimated by the method described in Mischi et al. (2012) for the transabdominal (a) and transrectal (b) ultrasound scans in the same patient presented in Figures 1 and 2. Both maps reveal the prostate extension into the bladder as angiogenic (*red color*).

As illustrated in Figure 2, reduced signal strength was observed in the transabdominal TICs. This could have resulted from the greater distance between the probe and the prostate; however, standard transabdominal probes, such as the one we used, are designed for imaging a large field of view rather than a small, deep target like the prostate. Probes dedicated to prostate imaging can be expected to produce better transabdominal prostate TICs.

The scanner settings were chosen on the basis of experience and real-time visual feedback, and improvements in image quality can be expected from a thorough, systematic optimization. Further improvements could also be achieved by optimizing the measurement protocol to account for the bladder volume, which can be adjusted by voiding. An empty bladder could result in increased attenuation from intestinal tissue in the ultrasound path, whereas a full bladder may result in non-linear propagation artifacts because of a long ultrasound propagation pathway through urine (Bouakaz et al. 2004). In general, at the adopted higher mechanical index, necessary for proper insonification of the peripheral zone in the

prostate, other effects may occur affecting the image quality, such as bubble destruction and non-linear propagation artifacts that can be observed independent of the amount of urine along the ultrasound path. Nevertheless, the quality of the TICs we obtained permitted analysis of the contrast agent bolus kinetics, as confirmed by our model-fitting evaluation.

With the size restrictions dictated by the transrectal route removed, the transabdominal approach facilitates the use of 4-D DCE-US, permitting analysis of the entire gland with a single intravenous UCA bolus. This would be an important improvement compared with 2-D imaging, where the analysis of each plane requires the injection of a separate UCA bolus.

Currently, DCE-US cannot replace the use of systematic biopsies for the diagnosis of PCa. However, recent studies have reported the emerging role of DCE-US in this context (Wink et al. 2008); biopsies targeted by DCE-US lead to fewer biopsies per session without compromise of detection rate compared with systematic biopsies (Mitterberger et al. 2007). Based on the preliminary results of quantitative methods, such as contrast ultrasound dispersion imaging (Kuenen et al. 2013b; Mischi et al. 2012), with a sensitivity and specificity of 77.3% and 86.0%, respectively (Kuenen et al. 2013a), further improvements can be expected in the localization of PCa by DCE-US. Especially when a high negative predictive value is achieved, abdominal DCE-US could be an easier, more comfortable option for selecting patients for biopsy, active surveillance and treatment monitoring and follow-up. Therefore, the proposed transabdominal DCE-US investigation could provide an important opportunity to limit biopsies in patients with a high suspicion of aggressive cancers.

In Figure 3 are the abdominal and TRUS functional dispersion maps for the same patient in Figures 1 and 2, estimated with the method proposed in Mischi et al. (2012). Both the transabdominal dispersion map and the corresponding TRUS map reveal the prostate extension into the bladder as highly angiogenic. This result, also supported by the 12-core biopsy, provides additional confidence in the feasibility of the transabdominal approach compared with TRUS. Other than the prostate extension into the bladder, visible in both scans, the images are not perfectly registered, because of the different ultrasound beam angles to the prostate from the abdominal wall and from the rectum.

CONCLUSIONS

We report the feasibility of transabdominal dynamic contrast-enhanced ultrasound imaging of the prostate, exploiting the lower ultrasound frequencies that are optimal for contrast-specific imaging. Time–intensity curves were successfully extracted and analyzed in 10 patients. Given the high incidence of prostate pathology, especially prostate cancer, together with the emerging role of dynamic contrast-enhanced ultrasound imaging for its localization, the use of the transabdominal approach to the prostate may represent a clinically useful option for selecting patients for biopsy, active surveillance and treatment monitoring and follow-up.

Acknowledgments—The authors are very thankful to David Cosgrove, Imperial College London (UK), for his valuable advice and contribution to the writing of this article.—This study was supported by (European Research Council) ERC Starting Grant 280209 and (Dutch Cancer Foundation) KWF Grant 2013-5941.

REFERENCES

Aarnink RG, Beerlage HP, De la Rosette JJ, Debruyne FM, Wijkstra H. Transrectal ultrasound of the prostate: Innovations and future applications. J Urol 1998;159:1568–1579.

Bouakaz A, Merks E, Lancee C, Bom N. Noninvasive bladder volume measurements based on non-linear wave distortion. Ultrasound Med Biol 2004;30:469–476.

Brown CT, O'Flynn E, Van Der Meulen J, Newman S, Mundy AR, Emberton M. The fear of prostate cancer in men with lower urinary tract symptoms: Should symptomatic men be screened? BJU Int 2003;91:30–32.

Draisma G, Boer R, Otto SJ, van der Cruijsen IW, Damhuis RA, Schröder FH, de Koning HJ. Lead times and overdetection due to prostate-specific antigen screening: estimates from the European Randomized Study of Screening for Prostate Cancer. J Natl Cancer Inst 2003;95:868–878.

Eckersley RJ, Sedelaar JP, Blomley MJ, Wijkstra H, deSouza NM, Cosgrove DO, de la Rosette JJ. Quantitative microbubble enhanced transrectal ultrasound as a tool for monitoring hormonal treatment of prostate carcinoma. Prostate 2002;51:256–267.

Fillon M. Contrast-enhanced ultrasound may aid prostate cancer detection. J Natl Cancer Inst 2013;105:444–446.

Frinking PJ, Bouakaz A, Kirkhorn J, Ten Cate FJ, de Jong N. Ultrasound contrast imaging: Current and new potential methods. Ultrasound Med Biol 2000;26:965–975.

Gorce JM, Arditi M, Schneider M. Influence of bubble size distribution on the echogenicity of ultrasound contrast agents: A study of SonoVue. Invest Radiol 2000;35:661–671.

Halpern EJ, Rosenberg M, Gomella LG. Prostate cancer: Contrast-enhanced US for detection. Radiology 2001;219:219–225.

Kuenen MP, Saidov TA, Wijkstra H, de la Rosette JJ, Mischi M. Spatiotemporal correlation of ultrasound contrast agent dilution curves for angiogenesis localization by dispersion imaging. IEEE Trans Ultrason Ferroelectr Freq Control 2013a;60:2665–2669.

Kuenen MP, Saidov TA, Wijkstra H, Mischi M. Contrast-ultrasound dispersion imaging for prostate cancer localization by improved spatiotemporal similarity analysis. Ultrasound Med Biol 2013b;39:1631–1641.

Kuenen MPJ, Mischi M, Wijkstra H. Contrast-ultrasound diffusion imaging for localization of prostate cancer. IEEE Trans Med Imaging 2011;30:1493–1502.

Menard S. Coefficients of determination for multiple logistic regression analysis. Am Stat 2000;54:17–24.

Mischi M, Jansen AH, Korsten HH. Identification of cardiovascular dilution systems by contrast ultrasound. Ultrasound Med Biol 2007;33:439–451.

Mischi M, Kalker T, Korsten E. Videodensitometric methods for cardiac output measurements. Eurasip J Adv Signal Process 2003;2003:479–489.

Mischi M, Kuenen MPJ, Wijkstra H. Angiogenesis imaging by spatiotemporal analysis of ultrasound contrast agent dispersion kinetics. IEEE Trans Ultrason Ferroelectr Freq Control 2012;59:621–629.

Mitterberger M, Horninger W, Pelzer A, Strasser H, Bartsch G, Moser P, Halpern EJ, Gradl J, Aigner F, Pallwein L, Frauscher F. A prospective randomized trial comparing contrast-enhanced targeted versus systematic ultrasound guided biopsies: Impact on prostate cancer detection. Prostate 2007;67:1537–1542.

Piscaglia F, Bolondi L, Italian Society for Ultrasound in Medicine and Biology (SIUMB), Study Group on Ultrasound Contrast Agents. The safety of Sonovue in abdominal applications: Retrospective analysis of 23188 investigations. Ultrasound Med Biol 2006;32:1369–1375.

Russo G, Mischi M, Scheepens W, De la Rosette JJ, Wijkstra H. Angiogenesis in prostate cancer: Onset, progression and imaging. BJU Int 2012;110:E794–E808.

Salomon G, Kollerman J, Thederan I, Chun FK, Budaus L, Schlomm T, Isbarn H, Heinzer H, Huland H, Graefen M. Evaluation of prostate cancer detection with ultrasound real-time elastography: A comparison with step section pathologic analysis after radical prostatectomy. Eur Urol 2008;54:1354–1362.

Schneider M. Characteristics of SonoVue. Echocardiography 1999;16:743–746.

Schröder FH, Hugosson J, Roobol MJ, Tammela TL, Ciatto S, Nelen V, Kwiatkowski M, Lujan M, Lilja H, Zappa M, Denis LJ, Recker F, Berenguer A, Määttänen L, Bangma CH, Aus G, Villers A, Rebillard X, van der Kwast T, Blijenberg BG, Moss SM, de Koning HJ, Auvinen A. Screening and prostate-cancer mortality in a randomized European study. N Engl J Med 2009;360:1320–1328.

Sedelaar JP, Vijverberg PL, De Reijke TM, de la Rosette JJ, Kil PJ, Braeckman JG, Hendrikx AJ. Transrectal ultrasound in the diagnosis of prostate cancer: State of the art and perspectives. Eur Urol 2001;40:275–284.

Siegel R, Ma J, Zou Z, Jemal A. Cancer statistics, 2014. CA Cancer J Clin 2014;64:9–29.

Strouthos C, Lampaskis M, Sboros V, McNeilly A, Averkiou M. Indicator dilution models for the quantification of micro-vascular blood flow with bolus administration of ultrasound contrast agents. IEEE Trans Ultrason Ferroelectr Freq Control 2010;57:1296–1310.

Wei JT, Calhoun E, Jacobsen SJ. Urologic Diseases in America Project: Benign prostatic hyperplasia. J Urol 2008;179:S75–S80.

Wink M, Frauscher F, Cosgrove D, Chapelon JY, Palwein L, Mitterberger M, Harvey C, Rouviere O, de la Rosette J, Wijkstra H. Contrast-enhanced ultrasound and prostate cancer: A multicentre European research coordination project. Eur Urol 2008;54:982–992.